

Trapping and Detrapping of Transport Carriers in Silicon Dioxide Under Optically Assisted Electron Injection

Hongseog Kim

Abstract— Based on uniform hot carrier injection (optically assisted electron injection) across the Si-SiO₂ interface into the gate insulator of n-channel IGFETs, the threshold voltage shifts associated with electron injection of $1.25 \times 10^{16} \text{ e/cm}^2$ between 0.5 and 7 MV/cm were found to decrease from positive to negative values, indicating both a decrease in trap cross section ($E_{ox} \geq 1.5 \text{ MV/cm}$) and the generation of FPC ($E_{ox} \geq 5 \text{ MV/cm}$). It was also found that FNC and large cross section NETs were generated for $E_{ox} \geq 5 \text{ MV/cm}$. Continuous, uniform low-field (1MV/cm) electron injection up to 10^{19} e/cm^2 is accompanied by a monotonic increase in threshold voltage. It was found that the data could be modeled more effectively by assuming that most of the threshold voltage shift could be ascribed to generated bulk defects which are generated and filled, or more likely, generated in a charged state. The injection method and conditions used in terms of injection fluence, injection density, and temperature, can have a dramatic impact on what is measured, and may have important implications on accelerated lifetime measurements.

Index Terms — ionizing radiation, optically assisted electron injection, FPC, FNC, NHTs, NETs

I. INTRODUCTION

As the dimensions of semiconductor devices decrease, the gate insulators of insulated gate field effect transistors (IGFETs) are subjected increasingly to processes involving ionizing radiation, such as reactive ion etching, e-beam evaporation, plasma-enhanced chemical vapor deposition (PECVD), x-ray lithography, e-beam lithography, and ion implantation.[1-6] All of these processes, either directly or indirectly expose the material being processed to substantial amounts of ionizing radiation. As a consequence, a number of electrically active defects can be formed in the gate insulators of IGFETs. Such defects would have a pronounced effect on the device characteristics of IGFETs, as well as on device long-term reliability. While much of the damage can be subsequently annealed, some of the defects may remain, and it is not known whether the annealed defects make the insulator more susceptible to additional damage, from either re-exposure to ionizing radiation or hot carrier stressing. It is also generally accepted that depending on how the gate insulator is prepared, the number and types of defects will vary. In any event, the highest quality gate insulators contain prodigious quantities of Neutral Hole Traps(NHTs), even when the devices have not been exposed to ionizing radiation.

Charged defects have an immediate effect on yield while charged and neutral defects affect lifetime (reliability). To determine their effects on lifetime, it is necessary to perform accelerated testing via hot carrier injection at an injection current density orders of magnitude larger than the oxide would ever be exposed

Manuscript received August 12, 2001; revised September 7, 2001.

The author is with Division of Information communication Engineering Paichai University Daejeon, Korea.
(e-mail : khsau@mail.paichai.ac.kr) Tel : +82-42-520-5868

to in normal operation.[7] The lifetime is then estimated from these results assuming the same degradation mechanisms are in play at the elevated stress level as in the normal operation of the device.

An effective procedure for studying electrically active bulk defects involves the uniform injection of a single carrier type across the substrate-oxide interface while monitoring the change in the threshold voltage, ΔV_t , or flatband voltage, V_{fb} , which is a measure of the fraction of these injected carriers that get trapped. Such an experiment emulates hot channel carrier injection and trapping, to a degree, but in a much more controlled fashion. Optically assisted injection is a relatively unaggressive implementation of such an approach, since it can be conducted at low oxide fields (1 MV/cm or less). In contrast, other methods, avalanche and Fowler-Nordheim injection, are much more aggressive, using oxide fields in excess of 7 MV/cm. The results of such injections, for threshold or flatband voltage shift vs the density of injected carriers, N_{inj} , whether via a non-aggressive or aggressive approach, are generally modeled using so-called first order trapping kinetics. Based on such modeling, trapping cross sections ranging from 10^{-13} – 10^{-20} cm² have been proposed in intrinsic state of the art insulators. Since cross sections of 10^{-17} cm² or less imply the existence of traps less than about 0.02 atomic dimensions, it is hard to reconcile such numbers with physical reality. This is especially so, since it is generally believed that electrically active insulator defects either gain or lose an electron or hole from atom sites.

Below evidence is presented that some of the very small cross section traps that have been identified may result from the measurement procedure creating bulk damage, as contrasted with simply measuring the damage. The fact that bulk defects can be generated during stressing is not new, since it has been observed at oxide fields >1.5MV/cm.[8-13] What is new is that it was observed: 1) charged bulk defect generation using a substrate hot electron injection technique at an oxide field of only 1MV/cm, 2) this generation is greatly enhanced at low temperatures, and 3) a simple model can be used to describe the data, rather than using a series of ever smaller cross section traps in a first order model. Additionally, it is believed that the defect generation at low oxide fields explains an unreported observation that

it previously could not be explained, namely the effect of the time to inject a given density of electrons on the magnitude of ΔV_t . This indicates that bulk defect generation is a function of the injection current density at the low oxide field employed here. At higher fields, >5MV/cm, it has been reported that the trap generation rate is proportional to the injection current density.[9] The fact that charged bulk defect generation rate is a function of the injection current density has dramatic implications on the validity of accelerated testing, using either high or low field techniques, to determine device lifetimes, which will be discussed elsewhere.[14]

II. EXPERIMENTAL PROCEDURES

Sample Preparation - Polysilicon IGFETs fabricated on 0.5 Ω ·cm (100), p-type substrates, were used. These devices had a gate insulator area of 5×10^{-4} cm² (width = 1000 μ m, length = 50 μ m), a gate insulator thickness of 36.1 nm, and are of the closed variety. The gate oxides used in this paper, are considerably thick, because it could clearly enable to investigate the defect behavior. The large gate area was used to facilitate the monitoring of the injection current density accurately. The gate oxides were thermally grown at 800°C in dry oxygen containing 4.5% HCl. All of the fabricated wafers were post-metal annealed at 400°C in H₂ for 30 min.

Threshold voltages (V_t) were determined by extrapolating the linear region of the drain-to-source current, I_{ds} , versus gate-to-source voltage, V_{gs} , curve at a drain-to-source voltage, V_{ds} , of 0.1 V and a substrate-to-source bias, V_{ss} , of -1 V. The I-V characteristic of each device was measured to determine its initial V_t . Electron injections were performed using a modified version of the optically assisted injection techniques. The threshold voltage was then remeasured, and ΔV_t due to electron trapping was obtained.

Optically Assisted Electron Injection - The configuration of the optically assisted electron injection is shown in Fig. 1.[15, 16] The gate-to-source/drain bias, V_{gs} , was applied to build up the electrical field across the gate insulator. The combination of gate-to-source and substrate-to-source bias, V_{ss} , was applied so as to form a depletion region. The electron-hole pairs were generated at the depletion region by the assistance of incident

white light. The electrons and holes were accelerated toward the Si-SiO₂ interface and substrate, respectively. If the energies of electrons were higher than the barrier height of the Si-SiO₂ interface, the electrons would enter the gate insulator and either be trapped at defects or pass through the gate oxide. The injected electrons passing through the gate insulator were measured by an electrometer. These measured electrons were approximately the same as the electrons injected at the Si-SiO₂ interface provided that the number of electrons being trapped in the gate insulator was much smaller than the number of electrons injected.

This technique enables the independent control of the electric field in the gate oxide and of the injection rate by using a combination of substrate bias and light intensity to control the injection rate.

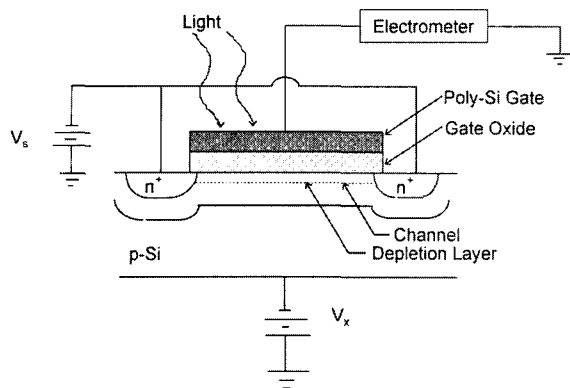


Fig. 1. Optically assisted electron injection system.

Two Level Injection - To study gate oxide field effects, the gate bias applied during the injection was varied such that the oxide field ranged from 0.5 to 7.0 MV/cm, assuming the devices were on. A "fresh" device was used at each oxide field. Electrons were injected at two different levels following determination of a device's initial V_t . First, a device was injected with approximately $2.5 \times 10^{13} \text{ e/cm}^2$ (referred to as a low level injection, or LLI), the fluence nominally employed to annihilate FPC(Fixed Positive Charge) ($\sigma \sim 10^{-13} \text{ cm}^2$). [17] V_t was remeasured and ΔV_t was determined. Then, an additional $1.25 \times 10^{16} \text{ e/cm}^2$ (referred to as a high level injection, or HLI), the fluence nominally used to label essentially all of large cross section NETs(Neutral Electron Traps) ($\sigma \sim 10^{-16} \text{ cm}^2$), were injected in the same

devices. V_t was remeasured again, and any additional ΔV_t was determined. The substrate biases applied were -7 V during the LLI and -16 V during the HLI. The injection current density was adjusted by changing the light intensity to yield a total injection time of 1~2 minutes for each injection level. Clearly, the injection of $1.25 \times 10^{16} \text{ e/cm}^2$ was at a much greater rate than that of $2.5 \times 10^{13} \text{ e/cm}^2$. Following two level injections at the varying oxide fields specified, the devices were reinjected at $E_{ox} = 0.7 \text{ MV/cm}$ and $V_{xs} = -7$ and -16 V, respectively, V_t was remeasured after each injection and additional ΔV_t from each injection was determined. In this way, any FPCs or large cross section NETs that remained unfilled or were generated, during the high field injections would now be filled and could be quantified.[8] From the first publication[16] dealing with defect quantification using two level optically assisted injection, and continuing into the present study, the same V_{xs} , -7 V for FPCs and -16 V for NETs and $E_{ox} = 0.7 \text{ MV/cm}$ have been employed. It has been recognized for a long time that using this procedure, specifically for quantifying NETs in unirradiated devices, that the devices were often "off" at the high substrate bias. However, staying with these biases enabled comparison of experiments conducted at different times on similar devices.

"Continuous" Injection - The "continuous" injections were performed automatically by injecting electrons in required number of increments over an injection range and were approximately evenly spaced on a log N_{inj} scale. For continuous injections, a constant substrate bias of -11 V and an applied oxide field of 1 MV/cm was used throughout generally for two reasons. The first of those was to keep the device on, and the second was to maintain a constant defect generation rate. In between each of these injections the I-V characteristic was measured to determine ΔV_t . Each I-V sweep takes less than one minute. ΔV_t was then plotted as a function of the cumulative number of injected electrons. From these "continuous" injection data, electron capture cross sections and densities were obtained by applying a least squared error fit of the equation of the electron trapping model.[16, 18]

III. MODEL

First Order Trapping Model - In order to understand

the effects of charge trapping, defects are typically characterized in terms of their capture cross section, σ , and density, N_T . To determine N_T and, 1st order trapping kinetics have been used to model electron trapping in the gate insulators of IGFETs. In this model, it is assumed that a trap can be occupied by only one electron, that its cross section and density are constant, that the trapping probability is $\ll 1$ (the current density is constant through the oxide), that the depopulation rate is insignificant compared to the population rate, that the injected carriers are non-interacting, and that the traps are non-interacting. From 1st order trapping kinetics, it can be shown that for a single type of trap, ΔV_t as a function of the density of injected electrons, N_{inj} , can be expressed as

$$\Delta V_t = \frac{qN_T\bar{x}}{\epsilon_{0X}} [1 - e^{-\sigma N_{inj}}], \quad (1)$$

where

$$N_{inj} = \frac{1}{q} \int_0^t J_G(t') dt', \quad (2)$$

σ and N_T are the cross section and areal density of the trap, respectively, J_G is the injection current density at the Si-SiO₂ interface, ϵ_{0X} is the permittivity of the oxide, and \bar{x} is the charge centroid measured from the gate electrode. Eq. (2) accommodates the filling of only a single type of trap, and requires that the total number of such traps (filled plus unfilled) be a constant. If more than one type of trap is present over the range of data acquired, the total change, ΔV_t , would be the sum of two or more equations of the type described in Eq. (2) as

$$\Delta V_t = \frac{q}{\epsilon_{0X}} \sum_{i=1}^n N_{T,i} \bar{x}_i [1 - e^{-\sigma_i N_{inj}}], \quad (3)$$

While in general the centroid for each type of trap could be different, using the wrong centroid would only yield a different density and would not affect the ability of the model to accurately represent the data. For the work presented here, it is assumed that the centroid is equal to the oxide thickness for all traps. It is known from past work[8] that the charge centroid of ionizing radiation induced fixed FPC, and large NETs, is about 6 – 8 nm

from the substrate-oxide interface.

Charged Bulk Defect Generation - Very little has been done to model charged bulk defect generation as a function of N_{inj} for substrate hot electron injection. It has been modeled only using a linear term[9] with limited success, but such a model was found inadequate for the present data. What was found to work well is a power law model. A power law has been used to describe interface state,[12, 19, 20] and bulk charge buildup during channel hot carrier injection, but has not been employed to model bulk defect generation resulting from uniform substrate hot electron injection. This model have been chosen to express in terms of N_{inj} , to be consistent with the first order model, as

$$\Delta V_t = \frac{q}{\epsilon_{0X}} \bar{x}_g a N_{inj}^b, \quad (4)$$

where a and b are the parameters of the model and are most likely to be a function of the injection current density and the oxide field. In general, \bar{x}_g in this equation is the centroid of the generated charge and could be different from the centroid of the other traps. For the work presented here, it is assumed that \bar{x}_g is equal to the oxide thickness. It should be noted that charge pumping measurements were made on these devices which show that the threshold voltage shift that was observed is not due to interface state build up.

In cases were there might be both existing traps and generation of new charged defects, a combination of the two models can be used by simply adding Eqs. (3) and (4) and to give the general equation

$$\Delta V_t = \frac{q}{\epsilon_{0X}} \{ \bar{x}_g a N_{inj}^b + \sum_{i=1}^n N_{T,i} \bar{x}_i [1 - e^{-\sigma_i N_{inj}}] \}, \quad (5)$$

This assumes that the two mechanisms are independent of each other. The procedure used to model a given set of ΔV_t vs N_{inj} data was to least squared errors fit Eqs. (3), (4), (5) and independently, and to compare the adequacy of the fit by choosing the simplest model that best fit the data. If a single charge generation term is employed and it fits the data over a range of N_{inj} which would require specification of several cross sections in a 1st order model, then one could argue that a single defect is generated. This is speculated

that the resulting fixed negative charge is the same as results when a NET traps an electron.

IV. RESULTS AND DISCUSSION

Effects of High Gate Insulator Fields on Unirradiated Devices - To study the effects of high gate insulator fields on unirradiated devices, electron injections at various fields, followed by reinjections at 0.7 MV/cm, were conducted, as described earlier. Fig. 2 shows the V_t of each device at each stage of the injection: 0) initial, prior to any injection, 1) following LLI at the field shown, 2) following HLI at the field shown, 3) following LLI at $E_{ox} = 0.7$ MV/cm, and 4) following HLI at $E_{ox} = 0.7$ MV/cm. Fig. 3 shows the incremental ΔV_t associated with each of the injections shown in Fig. 2, and is calculated by subtracting V_t before a particular injection from V_t after that injection. Thus, in Fig. 3, the curves shown are ΔV_t associated with: 1) LLI at the field shown, 2) a subsequent HLI at the field shown, 3) a subsequent LLI at $E_{ox} = 0.7$ MV/cm, and 4) a subsequent HLI at $E_{ox} = 0.7$ MV/cm.

It can be seen from curve 1 in Fig. 3 that the variation of ΔV_t with field is very small for the LLI. This is not unexpected, since the LLI should nominally fill only the FPCs present, very few are present in the unirradiated devices. Further, there is no direct evidence, as a consequence of this LLI, indicating the generation of FPCs which would manifest itself as V_t dropping below its initial value, curve 1 in Fig. 2.

A possible reason that FPCs are not generated during the LLI, independent of gate oxide field, is the low fluence of injected electrons used. This indicates high field alone cannot generate FPC, and that a high carrier injected fluence is also necessary. Unlike the LLI behavior, it can be seen from curve 2 in Fig. 3 that ΔV_t , for at-field HLI, decreases monotonically from positive to negative values. The decrease of ΔV_t from positive to zero in the range of E_{ox} between 1.5 and 5 MV/cm can be attributed to a decrease in the NET trap capture cross section which can be tested by a subsequent HLI at $E_{ox} = 0.7$ MV/cm, as discussed below. Since ΔV_t is zero for the preceding LLI, the negative values ΔV_t observed $E_{ox} \geq 5$ MV/cm due to the at-field HLI means that the resultant V_t must lie below its initial value, which is

readily observed in curve 2 in Fig. 2. This is compelling evidence indicative of the generation of FPCs. The presence of generated FPCs is further confirmed by the subsequent LLI at $E_{ox} = 0.7$ MV/cm. It is to be noted that FPCs could also have been created in the range of E_{ox} between 1.5 and 5 MV/cm. In this case, however, ΔV_t would remain positive, because a negative ΔV_t due to the formation of FPC does not dominate the positive ΔV_t due to the “labeling” of NETs.

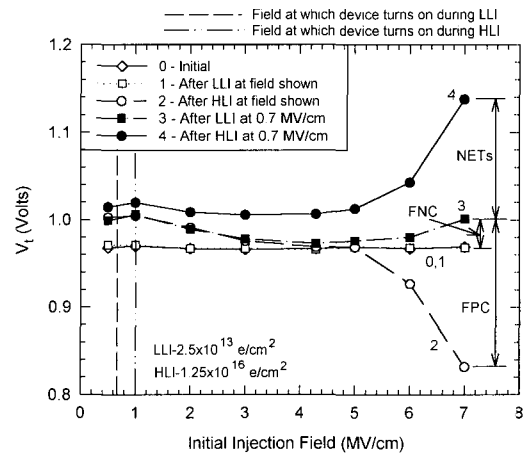


Fig. 2. Threshold voltage following LLI and high HLI at the field shown, and reinjection at $E_{ox} = 0.7$ MV/cm.

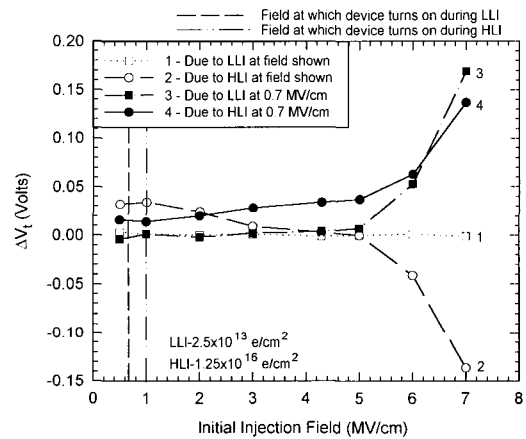


Fig. 3. ΔV_t following LLI and HLI at the field shown, and reinjection at $E_{ox} = 0.7$ MV/cm.

As mentioned above, the presence of generated FPCs was confirmed by a LLI reinjection, shown in Figs. 2 and 3, at $E_{ox} = 0.7$ MV/cm which would fill any FPCs which were not filled, or which were created during the high field injections. For unirradiated devices, there is no FPCs in uninjected device. Therefore, in Fig. 2, if there

is no generation of FPC during the high field HLI, V_i after the high field HLI (curve 2) should be the same as V_i after the 0.7 MV/cm LLI reinjection (curve 3) since this reinjection only injects enough carrier to fill FPCs that had not been previously filled. Note that curve 3 is the same as curve 2 up to $E_{ox} \approx 5$ MV/cm, and begins to deviate dramatically above 5 MV/cm. Thus, the reinjection supports the contention that FPCs were indeed generated during the high field HLI at fields > 5 MV/cm, and that no FPCs were generated at fields < 5 MV/cm.

From the above discussion, it can be concluded also that the creation mechanism is associated with a combination of injection fluence and oxide field, rather than field only. Building on this it can be argued that high field defect generation during injection is associated with carrier-defect site impact, and that because of low energies involved the damage is electronic rather than structural. While the creation mechanism for FPCs in the gate insulator oxide could be via impact ionization of injected carriers with neutral hole traps which are present in huge quantities in unirradiated gate insulators[21, 22], it could also be via band-gap ionization[23] and subsequent hole trapping in the neutral hole traps. If indeed, impact ionization is the mechanism responsible for the creation of FPCs in the gate oxide, the fact that they were not observed at 5 MV/cm and below is not surprising since at low fields the carrier would not become hot enough for impact ionization to take place. In fact, it is the maximum used in this work, indicating that direct impact ionization of a neutral hole trap is more likely responsible for the generation of FPCs. Such a creation model is consistent with the interrelationships between NHT, FPC, NET, and FNC(Fixed Negative Charge).[24] Another possibility is that hole injection from the anode, caused by the energetic electrons which reach this electrode, followed by hole trapping gives rise to the FPCs.

One additional observation can be made from the LLI reinjection at $E_{ox} = 0.7$ MV/cm, shown in Fig. 2 and 3. The fact that V_i following the LLI reinjection (curve 3) is above its initial value is evidence for the generation of FNCs. The creation mechanism for FNCs in the gate oxide can be explained by an analogous route to the high field formation of FPCs. Thus, if an NET captures an electron, a FNC is generated. Therefore, the presence of

FNCs following a high field HLI is not unexpected, since it simply means that some of the NETs captured an electron during the injection.

In addition to the creation of FPCs created during the at-field HLI, there is evidence that a large number of NETs are generated for $E_{ox} \geq 5$ MV/cm, and that their quantity does not saturate. This evidence is seen in curve 4 of Figs. 2 and 3, which show the V_i following a subsequent HLI reinjection at $E_{ox} = 0.7$ MV/cm, and the associated ΔV_i , respectively. This observation is consistent with those of DiMaria *et al.*[23] who claim that at fields as low as 4 MV/cm, NETs begin to be generated at an injected fluence of 6.2×10^{15} e/cm². Thus it is seen that the oxide field is a higher than Thompson.[13] It is believed the difference in these generation threshold fields can be attributed to the fact that the electron fluences which were employed in these earlier works, at fields used, were higher than those used in the present study. This is a direct result of the field that the generation rate increases with increasing oxide field, which would imply that the oxide field needed to observe defect creation would increase as the injected charge is decreased. Such an explanation is consistent with the field needed to create defects as the amount of injected charge is decreased. The use of different injected electron fluences in the present work, and in the earlier referenced studies,[10, 13] explains the different ΔV_i behavior observed as a function of oxide field.

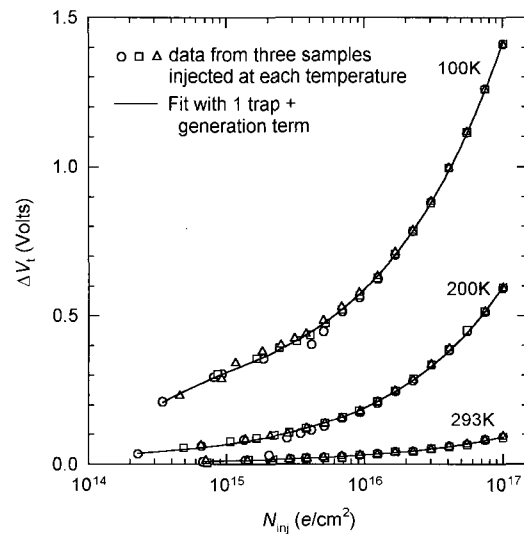


Fig. 4. ΔV_i vs N_{inj} during electron injection at 293, 200, and 100K.

Table 1. Least squares fitting parameters using generation + one 1st order trap at 293, 200, and 100K.

T(K)	Generation Model ($N_F = aN_{inj}^b$)		Trap 1 - NET	
	a	b	$N_T(\text{cm}^{-2})$	$\sigma(\text{cm}^2)$
293	2.1×10^2	0.495	0.1×10^{10}	2.5×10^{-15}
200	4.9×10^2	0.521	0.8×10^{10}	9.7×10^{-15}
100	5.9×10^3	0.477	10.0×10^{10}	3.6×10^{-15}

Figure 4 shows the variation of ΔV_t vs N_{inj} measured at 293, 200, and 100K for the IGFETs used here. The data points represent actual experimental data points and the solid lines are the fits to the data using generation term plus one 1st order trap. The parameters for the models used in Fig. 4 are given in Table 1. To see if interface states generation could be affecting the measurements, charge pumping measurements were done to characterize the interface traps before and after injection at each temperature. Before injection, mean interface state density was found to be $\sim 7 \times 10^9 \text{ cm}^{-2} \cdot \text{eV}^{-1}$ at mid-gap for each temperature. Mean interface state density was remeasured after injection and found to be 7×10^9 , 7.9×10^9 , and $9.8 \times 10^9 \text{ cm}^{-2} \cdot \text{eV}^{-1}$ at mid-gap for the injections performed at 293, 200, 100K, respectively. Thus, it would appear that interface state generation makes a negligible contribution to the ΔV_t given in the figure for these high quality “dry” oxides. It is perhaps of interest to note that while these are not steam oxides, they are not really dry since HCl was employed in their growth and no attempt was made to preclude incorporation of H₂O from the ambient atmosphere during or after fabrication in a Class 1 cleanroom.

From the 100K data, and to a lesser degree the 200K data, shown in Fig. 4, the question does arise as to whether there really is a 1st order trap that is being seen for the low N_{inj} , or is it just an inaccuracy in the measurement, and bulk charged defect generation is the only mechanism taking place. It is quite reasonable that as the temperature is lowered, a “shallow” trap that is not visible at room temperature will capture carriers. The cross section for this trap was determined to be $3.6 \times 10^{-15} \text{ cm}^2$, placing it in size between the FPCs and large cross section NETs, and two orders of magnitude larger than the so-called water related traps.

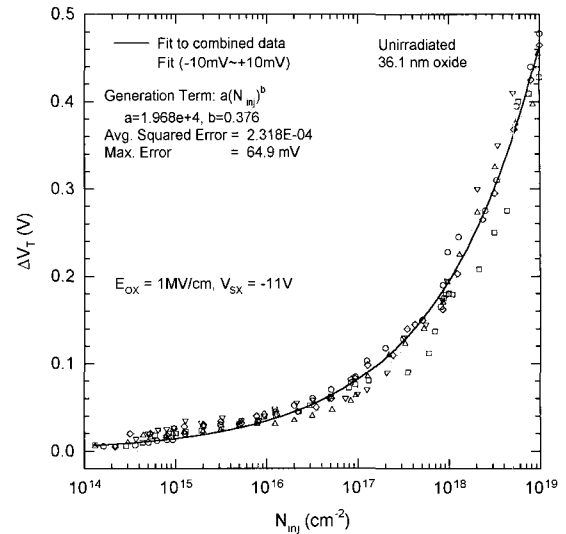


Fig. 5. ΔV_t vs N_{inj} during electron injection at room temperature. The solid lines are the fits to the data using only generation model.

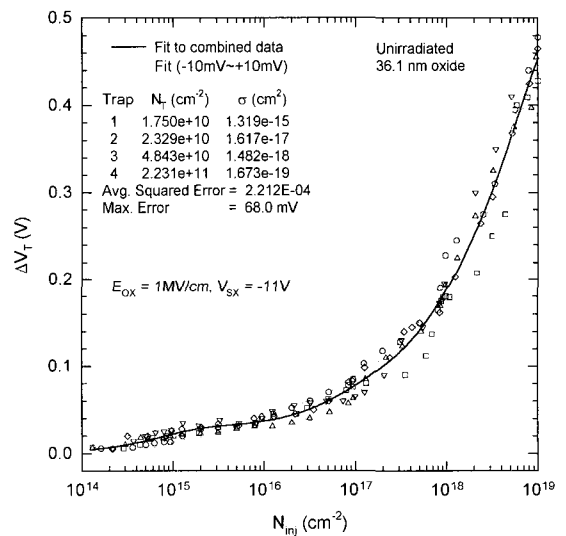


Fig. 6. ΔV_t vs N_{inj} during electron injection at room temperature. The solid lines are the fits to the data using four 1st order traps.

Using a series of trap cross sections to model the data is not without merit since oxides that have been exposed to ionizing radiation are known to have at least two distinct traps present, FPCs and large cross section NETs.[17] However, given the lack of “structure” in the present data above the mid 10^{15} e/cm^2 injected, it is difficult to justify using a three trap model, or even a two trap model. In either case, the derived cross sections include one in the 10^{-17} cm^2 range. This implies the existence of at least one trap with a capture cross section

of approximately 0.02 atomic dimensions which is difficult to explain. In some injection studies up to 10^{19} e/cm^2 at room temperature, where 4 cross sections are necessary to fit 1st order model, one trap and a generation term are the most needed. This is shown in Fig. 5 and 6.

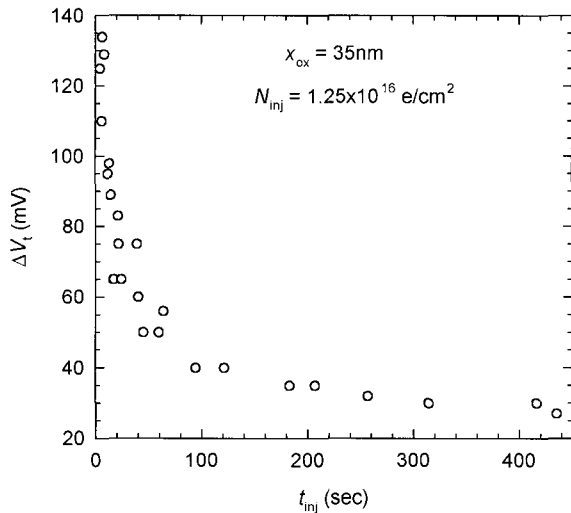


Fig. 7. ΔV_t vs t_{inj} to inject 1.25×10^{16} e/cm^2 into an IGFET with a 35 nm thick gate oxide.

An observation that it have been made for a number of years in investigating intrinsic and extrinsic large cross section NETs is that the ΔV_t measured for a given N_{inj} was a function of how rapidly the electrons were injected. Fig. 7 shows just such a measurement obtained by plotting ΔV_t vs the time to inject, t_{inj} , 1.25×10^{16} e/cm^2 for a 35 nm thick gate oxide device of the same type used in other studies in this work. It was assumed usually that the effect was due to depopulation. Based on the generation studies discussed and depopulation studies, it was believed that what was being observed was primarily due to detrapping, since the longer it took to inject the electrons, the longer those that had already trapped an electron would have to detrapp. This was supported by the fact that the effect was not observed in similar measurements of FPCs in an irradiated device, where detrapping is not expected, due to the coulombic attraction of the electron to the FPC site. An electron captured by a neutral site should be much easier to detrapp and that was happening. However, depopulation experiments on the devices did not at all account for the differences seen in Fig. 7 for different times of injection.

Then it was speculated that the discrepancy was due to non-uniform injection at the higher injection current density (shorter t_{inj}) even though there was no other proof.

V. CONCLUSION

The effects of injecting carriers at different gate insulator fields, on observed ΔV_t during optically assisted electron injection to quantify charged and neutral defect densities in unirradiated devices were examined. Since very few FPC are present in a high quality insulator, no ΔV_t was observed in a LLI for such devices. The threshold voltage shifts associated with an at-field HLI between 0.5 and 7 MV/cm were found to decrease from positive to negative values, indicating both a decrease in trap cross section ($E_{ox} \geq 1.5$ MV/cm) and the generation of FPC ($E_{ox} \geq 5$ MV/cm). It was also found that FNC and large cross section NETs were generated for $E_{ox} \geq 5$ MV/cm.

Also, it is necessary to find out the defect generation at low fields which was not observed using two level injection method. Continuous, uniform low-field electron injection across the Si-SiO₂ interface into the gate insulator of n-channel IGFETs using optically assisted hot electron injection of up to 10^{19} e/cm^2 is accompanied by a monatomic increase in threshold voltage. The threshold voltage shift as a function of the density of injected carriers can be modeled using first order trapping kinetics with several trapping cross section. However, such a model is difficult to justify given the lack of "structure" in the observed data and the fact that using such a model leads to the conclusion that one or more of the traps are subatomic in size, *i.e.* approximately 0.02 atomic dimensions. In fact, if the injection is continued beyond the 10^{19} e/cm^2 level, the threshold voltage shift continues unabated, requiring smaller and smaller assumed trapping cross section.

It was found that the data could be modeled more effectively by assuming that most of the threshold voltage shift could be ascribed to generated bulk defects which are generated and filled, or more likely, generated in a charged state. At room temperature, in fact, virtually all the observed threshold voltage shift appears to be due to charged bulk defect generation. As the temperature is

reduced, the data indicate that there is a single large cross section NET in addition to a large amount of bulk charged defect generation. Charge pumping measurements indicated that the shifts observed were not the result of interface state generation under the low field conditions employed.

This paper indicates that hot electron injection using any technique, but especially using more aggressive conditions (higher fields and/or current densities) than used, here not only results in the filling of existing traps, but also in the generation of charged bulk defects. Using more aggressive conditions enhances the generation of charged bulk defects, and can also result in the simultaneous generation of interface states. Therefore, questions about the validity of accelerated hot carrier reliability are raised. It also raises questions about the existence of extremely small traps, since the latter are characterized by applying first order trapping theory to data obtained by high field, high current density avalanche injection methods, which could very easily result in the generation of bulk defects of the kind discussed herein.

ACKNOWLEDGEMENTS

This study was financially supported by Paichai University for central research fund in 2001.

REFERENCES

- [1] C. K. Williams, A. Reisman, P. Bhattacharya, and W. Ng, *J. Apply. Phys.*, vol. 64, p. 1145, 1988.
- [2] C. K. Williams, A. Reisman, and P. Bhattacharya, *J. Apply. Phys.*, vol. 66, p. 379, 1989.
- [3] M. Walters and A. Reisman, *J. Apply. Phys.*, vol. 67, p. 2992, 1990.
- [4] C. T. Gabriel, *2001 6th Intl. Symp. Plasma Process-Induced Damage*, p. 20, 2001.
- [5] P. W. Mason, D. K. DeBusk, J. K. McDaniel, *2000 5th Intl. Symp. Plasma Process-Induced Damage*, p. 2, 2000.
- [6] J. W. Jung, S. B. Han, and Kyungho Lee, *J. Semiconductor Technology science* vol 1, p. 31, 2001.
- [7] I. Chen, J. Y. Choi, T. Chan, and C. Hu, *IEEE Trans. Electron Devices*, vol. 35, p. 2253, 1988.
- [8] R. Bright and A. Reisman, *J. Electrochem. Soc.*, vol. 140, p. 2065, 1993.
- [9] Y. Nissan-Cohen, J. Shappir, and D. Frohman-Bentchkowsky, *J. Apply. Phys.*, vol. 60, p. 2024, 1986.
- [10] D. J. DiMaria and J. W. Stasiak, *J. Apply. Phys.*, vol. 65, p. 2342, 1989.
- [11] C. C. H. Hsu, T. Nishida, and C. T. Sah, *J. Apply. Phys.*, vol. 63, p. 5882, 1988.
- [12] B. Doyle, M. Bourcerie, J. -C. Marchetaux, and A. Boudou, *IEEE Trans. Electron Dev.*, vol. 37, p. 744, 1990.
- [13] T. Nishida and S. E. Thompson, *J. Apply. Phys.*, vol. 69, p. 3986, 1991.
- [14] H. S. Kim, A. Reisman, and C. K. Williams, *J. Electrochem. Soc.*, vol. 144, p. 2517, 1997.
- [15] A. Reisman, C. K. Williams, and J. R. Maldonado, *J. Apply. Phys.*, vol. 62, p. 868, 1987.
- [16] T. H. Ning and H. N. Yu., *J. Apply. Phys.*, vol. 45, p. 5373, 1974.
- [17] T. H. Ning *J. Apply. Phys.*, vol. 49, p. 4077, 1978.
- [18] E. H. Nicollian, C. N. Berglund, P. F. Schmidt, and J. M. Andrews, *J. Apply. Phys.*, vol. 42, p. 5654, 1971.
- [19] C. Hu, S. C. Tam, F. -C. Hsu, P. -K. Ko, T -Y. Chen, and K. W. Terrill, *IEEE Trans. Electron Dev.*, vol. 32, p. 375, 1985.
- [20] R. Bellens, E. de Schrijver, G. Van den bosch, G. Groeseneken, P. Hermans, and H. E. Maes, *IEEE Trans. Electron Dev.*, vol. 41, p. 413, 1994.
- [21] L. Lipkin, A. Reisman, and C. K. Williams, *Apply. Phys. Lett.*, vol. 57, p. 2237, 1990.
- [22] T. H. Ning *J. Apply. Phys.*, vol. 47, p. 1079, 1976.
- [23] D. J. DiMaria, E. Cartier, and D. Arnold, *Appl. Phys. Lett.*, vol. 73, p. 3367, 1993.
- [24] M. Walters and A. Reisman, *J. Electrochem. Soc.*, vol. 38, p. 2576, 1991.



Hongseog Kim received the B.S. Degree in Electronics Engineering at Seoul National University, Seoul, Korea, in 1985, and the M.S. degree and the Ph.D. degree in Electrical Engineering at North Carolina State University, in 1989 and 1996, respectively.

Between 1996 and 1999, he was with LG Semicon Company, Ltd., Cheongju-si, Korea, where he involved in Advance Dram Development Team, as a senior research engineer. In 1999, he joined the Hyundai Electronics Company, Ltd., and had been engaged in the development of 0.16 μ m technology DRAM's. In 2000, he joined Division of Information Communication Engineering at Paichai University, Taejon, Korea, as an assistance professor. His current research interests include the device design, the device reliability, and RF circuits.